Proceedings of the 2003 IEEE
International Conference on Robotics & Automation
Taipei, Taiwan, September 14-19, 2003

Touching Stomach by Air

Makoto KANEKO*, Tomohiro KAWAHARA*, Satoshi MATSUNAGA*
Toshio TSUJI*, and Shinji TANAKA**

*Graduate School of Engineering, Hiroshima University, Higashi-Hiroshima, JAPAN
**Graduate School of Biomedical Sciences, Hiroshima University, Hiroshima, JAPAN

Abstract

This paper proposes a new endoscope system with an air injection based contact probe capable of measuring the local impedance of the inner surface of stomach. By utilizing air pressure, we can produce an equivalent contact force, which is really advantageous for avoiding any damage for stomach during an examination. A big issue is that there is no way to obtain the applied force to stomach exactly. The key for solving it is the specially designed solenoid valve with the response of more than 500Hz. The solenoid valve with such a high response allows us to estimate each impedance parameter, even with a reference value. We show experimental system with a couple of interesting results.

Key words: *Tactile Probe, Endoscope, Impedance, Air pressure, High speed valve*

1 Introduction

Both endoscope camera and ultrasonic probe are well known tools for examining an early stage of cancer of stomach. The endoscope camera provides us with visual information of the inner surface of stomach. Due to the direct observation, it is the most convenient tool for examining cancer, especially located at the inner surface. On the other hand, there are some cases where a cancer cannot be clearly observed by endoscope camera, while there may exist cancer cells behind the surface of stomach. The ultrasonic probe enables us to detect candidates of cancer cells through the density information of stomach, even under the case where an endoscope camera fails in catching visually. Even utilization of both endoscope and ultrasonic probes is not still perfect for finding cancer cells and there are still many cases where we fail in catching them successfully through examinations. Some medical doctors are pointing out that they should measure the local stiffness of stomach so that they may increase the quality for examination. The tissue suffered by cancer is generally high stiffness compared with the other parts which are not attacked by cancer.

As well known, an endoscope system is normally composed of a flexible tube controlled by wires, a stereo camera, fiber cables for guiding lightening signal, and a forceps if necessary. Forceps is often used for picking up a sample from the surface of stomach or for removing a particular polyp. In order to feel the local stiffness of such tissue, some medical doctors try to push the tip of forceps to the tissue, as shown in Fig. 1(a), where fingers can directly feel the sensation of stiffness. However, since there exists non-negligible contact friction between the flexible tube and the forceps, fingers can not feel the right sensation of the local stiffness of tissue. Furthermore, the contact friction between two mechanical components heavily varies according to the curvature of the flexible tube, which makes a different sensation of stiffness for a real one. An alternative way to obtain the local stiffness is to implement both a position sensor at the grasping point and a force sensor at the tip of forceps, as shown in Fig. 1(b). The local stiffness can be obtained by dividing the force increase by the position displacement of rod. Furthermore, if we implement one more force sensor at the grasping point, we can always compensate the contact friction between the flexible tube and the forceps by utilizing an appropriate power assist system, although it is a bit dangerous since the power assist system

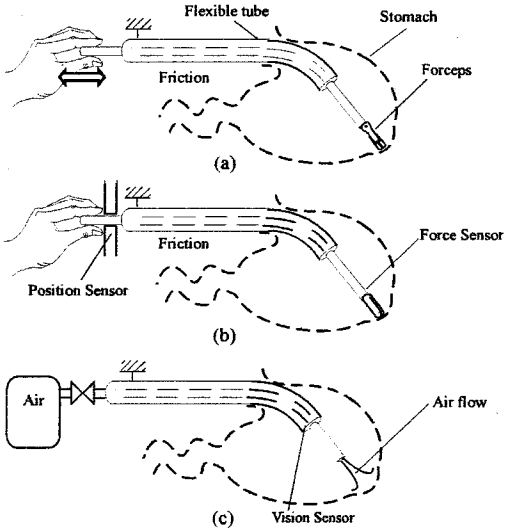

Fig. 1: Three approaches for touching stomach

may produce an unexpectedly large force to the stomach. Since these approaches touch the stomach directly by a mechanical rod, patients can never feel comfortable and moreover, they may not be good from the viewpoint of safety. This work is strongly motivated by these backgrounds. The key idea is to produce an equivalent contact force by air flow as shown in Fig. 1(c), where the local displacement of the inner surface can be measured by either a stereo vision naturally equipped with an endoscope or a laser sensor newly implemented. We would note that the goal of this paper is to provide a method for measuring the impedance by applying a virtual force through air pressure. Fig. 2 shows an overview of the proposed system where the air supply system surrounded by the real line is the only equipment additionally implemented to a conventional endoscope. Such an indirect contact method is really advantageous for avoiding any damage for stomach during an examination. A big issue, however, is that there is no way to obtain the exact applied force to the tissue to be measured. To cope with this issue, we measure the relationship between the applied force and the distance up to the object in advance. By preparing such calibration data, we can estimate the contact force by simply measuring the distance between the nozzle hole of endoscope and the tissue. The estimated force is utilized for computing the local impedance with a combination of distance measured by a vision sensor. Increasing resolution is, of course, an important issue for medical application, since a rough resolution can not catch candidates of cancer cell. High resolution will be kept by narrowing the area where the air flow can touch. We attach the air nozzle whose diameter is $2mm$ so that we can make the contact area narrow. Also, the air valve is a key component for quickly switching the air pressure with respect to the input signal. The specially designed air valve with the official response of $500Hz$ is included in the air supply system. Such an air valve allows us to obtain not only the stiffness but also dynamic related parameters, such as a damping coefficient and an equivalent mass of tissue. This paper shows a couple of preliminary results to explore the basic working principle on air pressure based active sensing for measuring mechanical impedance. We design and develop the experimental system composed of air supply system with the high speed valve, a driver for controlling the valve, a dummy pipe with nozzle, a laser distance sensor, and a PC for sending the control data to the driver as well as for analyzing the data obtained. By utilizing the system, we execute a couple of experiments for confirming whether the proposed method can successfully estimate the mechanical impedance for test pieces or not.

After briefly reviewing related works, we first introduce the basic structure of the proposed sensor system in section 3 where both the air valve and the basic working principle are precisely described. In section 4, we show a couple of experimental results to verify the basic idea. For a future direction, we add some discussions in section 5 before concluding remarks.

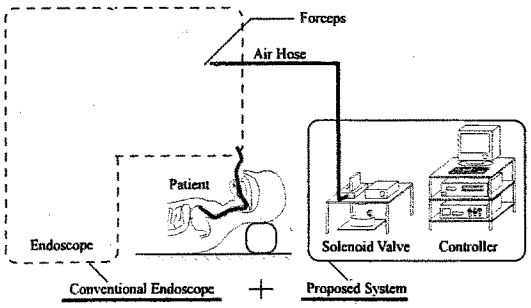

Fig. 2: The proposed system

2 Related Works

There have been many works [1]-[7] discussing medical robots, such as minimum invasive surgery, brain surgery, bone surgery in joint, and so forth. Catheter is a good tool for diagnosing inner surface of stomach, large intestine, and so forth. Most catheters include vision, so that they can observe inside of the surface of internal organs. Training how to manipulate catheters is a big issue especially for students majoring surgeon. Ikuta and others have provided with a training system by applying the technology of master-slave tele-operation in robotics [8].

As for sensing mechanical impedance of living things, Hogan and his group have first challenged to measure the stiffness of human muscle, especially by focusing on arm [9]. Tsuji and his group have precisely measured the mechanical impedance of human arm by imparting a quick active motion to the hand compulsively [10]. They computed the impedance from both the force and the position data at hand with respect to time. Howe et al. and Kawamura et al. have measured the impedance of finger tip. Sensing mechanical impedance definitely needs active motion, otherwise the impedance parameters can never be obtained. There are two ways to produce an active motion; one is the direct contact method and the other is based on non-contact method. Most works so far proposed can be categorized into the group of direct contact method. It has the potential capability for accurately obtaining each parameter. This is because we can measure the contact force accurately through the direct contact between the sensor rod and the target. On the other hand, there are various situations where we are obliged to take the non-contact method. Such a situation may happen either when keeping sanitary is a big priority or when the target is fragile for an excessive force. The needs for such a non-contact method is perhaps for measuring the freshness of law fish and vegetable or examining the youth through the stiffness of skin, while the accuracy will be surely less than that of the direct method. As for non-direct method, Shinoda and Yamazaki have proposed the surface hardness evaluation based on acoustics of air in the space between sensor and

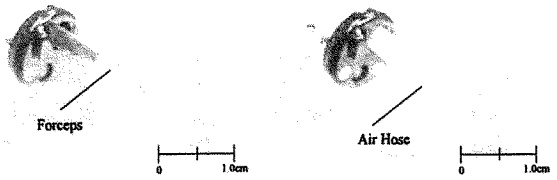

(a) Forceps (b) Hose

Fig. 3: End face of endoscope

object surface [11],[12]. They utilized speakers for producing an input to the object and a microphone for picking up the output coming from the acoustic impedance between the sensor and the object. While this is the first challenge on non-direct impedance measurement, the utilization of both speaker and microphone strongly makes limitation for its use due to its weak force generation. For stomach diagnosis, it may be necessary to obtain the impedance parameters not only for the surface but also for some distance from the surface, which means that a pretty large pushing force must be necessary during sensing. This is the reason why we utilize the air pressure based non-contact approach for our purpose. By utilizing the air pressure, we can apply an enough force to obtain a large displacement enabling us to evaluate an impedance at some distance from the surface.

3 Basic Working Principle

While the inner surface of stomach, of course, exhibits highly nonlinear behavior, we suppose a linear mechanical system composed of mass m, damper c and spring k. This assumption is valid for a small displacement, since we can make linearization around an equilibrium point even for the object with non-linear behavior. With this assumption, the equation of motion is given by,

$$m\ddot{x} + c\dot{x} + kx = f(t) \tag{1}$$

We can measure the displacement x by a vision sensor, and both $\ddot{x}$ and $\dot{x}$ are numerically computed with combination of an appropriate low pass filter. For data processing, there are two keys; filtering without time delay and the calibration map of $f(t)$. The data after a low pass filter have a delay compared for the original data. Such a delay is not desirable for accurate estimation of impedance parameter, since we can not utilize $\ddot{x}$, $\dot{x}$, and x at the same time frame. To cope with this, two times filtering are done for each derivative for adjusting time. We first apply the forward filtering where it is executed for the positive direction of time, and then apply the backward filtering where it is achieved for the negative direction, so that we can avoid any time lag for both $\ddot{x}$ and $\dot{x}$. Generally, the applied force $f(t)$ can not be measured directly for non-contact approach. In our approach, $f(t)$ can be regarded as a function of the distance up to the object and the pressure at air tank. We calibrate $f(t)$ with respect to distance and pressure in advance and utilize the calibration map for analysis. For n sets of data, we can obtain the following set,

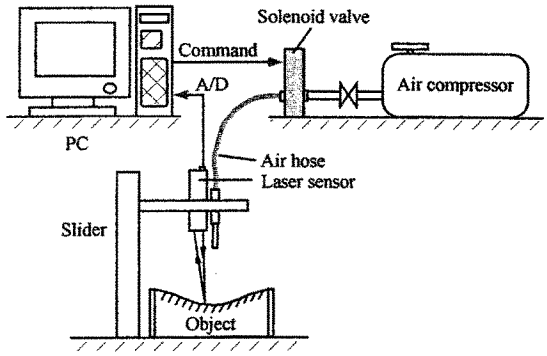

Fig. 4: Experimental system

$$Az = v \tag{2}$$

where $z = [m, c, k]^T$, $v = [f_1, f_2, \cdots, f_n]^T$, and

$$A = \begin{bmatrix} \ddot{x}_1 & \dot{x}_1 & x_1 \\ \ddot{x}_2 & \dot{x}_2 & x_2 \\ \vdots & \vdots & \vdots \\ \ddot{x}_n & \dot{x}_n & x_n \end{bmatrix} \tag{3}$$

By using the seudo-inverse matrix $A^{\#}$of A, we can obtain the least-square solution of eq. (2) by eq. (4)

$$z = A^{\#}v \tag{4}$$

where $A^{\#} = (A^T A)^{-1} A^T$.

4 Experiments

4.1 Experimental system

Fig. 3 shows the end face of endoscope where a hole is prepared for inserting a forceps. A doctor manually controls it for taking a sample of tissue or for partially removing it. Our idea is to utilize the hole for air supply, so that we can use the most of conventional endoscope system. Fig. 3(b) shows an image where instead of inserting a forceps, a hose is inserted into the hole for supplying air. In order to execute basic experiments, we simply pick up the hose without the endoscope and construct the air supply system for testing. Fig. 4 shows the experimental system where it is composed of an air hose, a specially designed solenoid valve, a driver for controlling the valve, an air compressor for producing compressed air, a laser sensor for measuring the distance up to the object, a two-axis slider

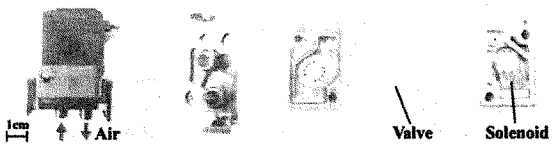

Fig. 5: Components of solenoid valve

for moving the probe, and a PC for taking in data as well as managing the whole system. The key component is the specially designed solenoid valve whose maximum switching frequency is $500Hz$. Fig. 5 shows an overview of the valve composed of an electro-magnetic element for generating high frequency, a valve with the mass of $40g$, and the case for packing those two components. The valve has no spring element and the equivalent effect is generated by air. The valve is controlled by two parameters, namely, time period and duty factor denoting the ratio between ON time and the time period. The applied force can be controlled either by changing the pressure of the air compressor or by changing the duty factor. For example, the step response can be achieved by the duty factor of unity.

4.2 Preliminary Experiments

Fig. 6(a) shows the preliminary experiments for examining how the air flow spread with respect to the distance up to the object, where p, p_{max}, b, and b_1 are the local pressure, the maximum pressure, the length perpendicular to the flow axis, and the width where the pressure results in half of p_{max}, respectively, and symbols indicated by Δ, $\bullet$, and $\square$ are the data corresponding to the distance between the nozzle and the object shown in the figure, respectively. These parameters have been often utilized for representing the velocity profile spreading from a nozzle [13]. From Fig. 6(a), we can see that there exists a weak similarity between p/p_{max} and b/b_1. This means that if we can measure the distance up to the object and p_{max}, we can obtain a rough pressure profile and as a result, we can evaluate the applied force by integrating the pressure profile. Fig. 6(b) shows the relationship between the generated force and the distance up to the object. From Fig. 6(b), we can see that the force does not much change according to the distance. This means that we can regard the applied force constant with respect to the distance, while the equivalent contact area changes. Fig. 6(c) shows an example of time history of the applied pressure for a step response, where the noise appearing in the data perhaps comes from the sensor but not from the flow turbulence. From Fig. 6(c), we would note that the step response itself is quick enough to make sure that we can utilize the ideal step response instead of the actual force signal. Such a quick response comes from the high response of the solenoid valve.

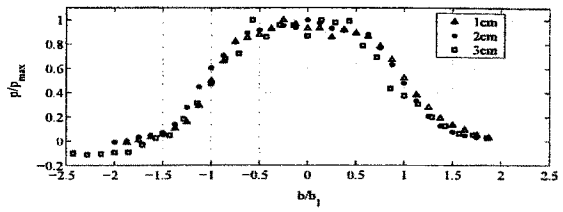

(a) Pressure distribution

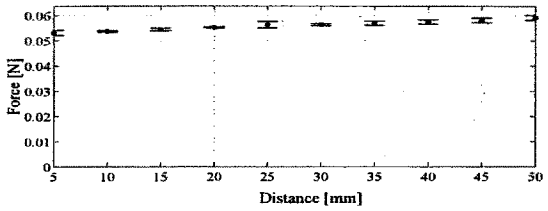

(b) Force with respect to distance

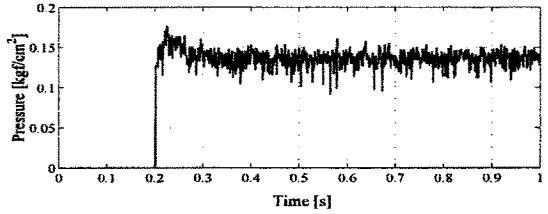

(c) Step response

Fig. 6: Preliminary experiments

4.3 Experimental Results

Fig. 7 shows experimental results for three different environments where both (a) and (b) exhibit overshooting behaviors with small damping coefficient, and (c) is an overdamping behavior with a pretty large damping coefficient, where the mark " $\wedge$ " denotes the estimated value. The air pressure is stepwisely imparted to the plate at a particular point and the displacement at the point is measured by a laser sensor until the response comes to rest. Fig. 7(a-1), (a-2) and (a-3) show the time histories of the measured displacement, the computed displacement based on eq.(1) with the impedance parameters estimated by the measured force data, and the computed displacement also based on eq.(1) with the impedance parameters estimated by the commanded force, respectively. Although the force signal includes much noise as shown in Fig. 6(c), the estimated parameters are not much different between (a-2) and (a-3). All displacement signals in Fig. 7(a) finally converge to the same point, which means that the stiffness is at least well estimated for both (a-2) and (a-3). From the beautiful coincidence of time period for all displacement signals, we can naturally expect that the mass is also well estimated in both (a-2) and (a-3). However, the coinci-

dence of damping coefficient between both (a-2) and (a-3) is not as good as that of either stiffness or mass, and there exists 25% difference in damping coefficient between them. The noise included in the force signal makes the estimation of damping coefficient difficult, which can be observed by the difference of behaviors between (a-1) and (a-2). On the other hand, we can see that the coincidence between (a-1) and (a-3) is nicer than that between (a-1) and (a-2). This observation suggests that we are allowed to utilize the commanded force instead of the measured one. In Fig. 7(b), we put the tip of plate in liquid, so that we can increase damping. It can be seen from Fig. 7(b-1) and (b-2) that the computed position based on the estimated data is nicely fit to the measured one. This implicitly ensures the nice estimation of impedance parameters for such a pattern. We would note that the estimated mass is almost two times lager than that in Fig. 7(a-3). This is because putting the tip of the plate in liquid increases an equivalent mass. In Fig. 7(c), we put the tip of plate in liquid with a further viscosity. From Fig. 7(c-1) and (c-2), we can see that the coincidence between the actual and the estimated displacements is fairly good while the estimation of mass is terribly small. This is because an ideal response itself is not sensitive for the change of mass for such an overdamping behavior, as shown in Fig. 8, where both responses do not have much difference while they have hundred times different mass each other. This means that we have to be very careful for estimating impedance parameters when the displacement signal has an overdamping behavior.

5 Discussions

Surface of stomach may be modeled by just like a rubber. Fig. 9 shows a test piece made by a balloon where we partially change the thickness so that we can purposely change the stiffness. Without such a change, we can find the smallest stiffness at the center, while it gradually increases toward the edge under uniform material. The point shown by no.2 has a thin thickness locally so that we can purposely obtain a low stiffness at the particular point. Fig. 10 shows how the natural frequency changes with respect to the position, where a laser doppler sensor is utilized for this particular experiment. There are three oscillating modes where the smallest one corresponds to the local oscillation mode at point2, the middle one corresponds to the fundamental oscillation mode of the rubber, and the highest one the second oscillation mode, respectively. When imparting a sinusoidal input to the center (no.3), we can expect a large power for the fundamental oscillation mode. When giving the same input near the edge, we expect a large power for the second oscillation mode. Also, if we impart such an input to the point 2, we can expect a large power for the lowest oscillation mode. An interesting observation in Fig. 10 is that the peak power changes according to the force applying point and the actual behavior perfectly matches with those expected by the above considerations.

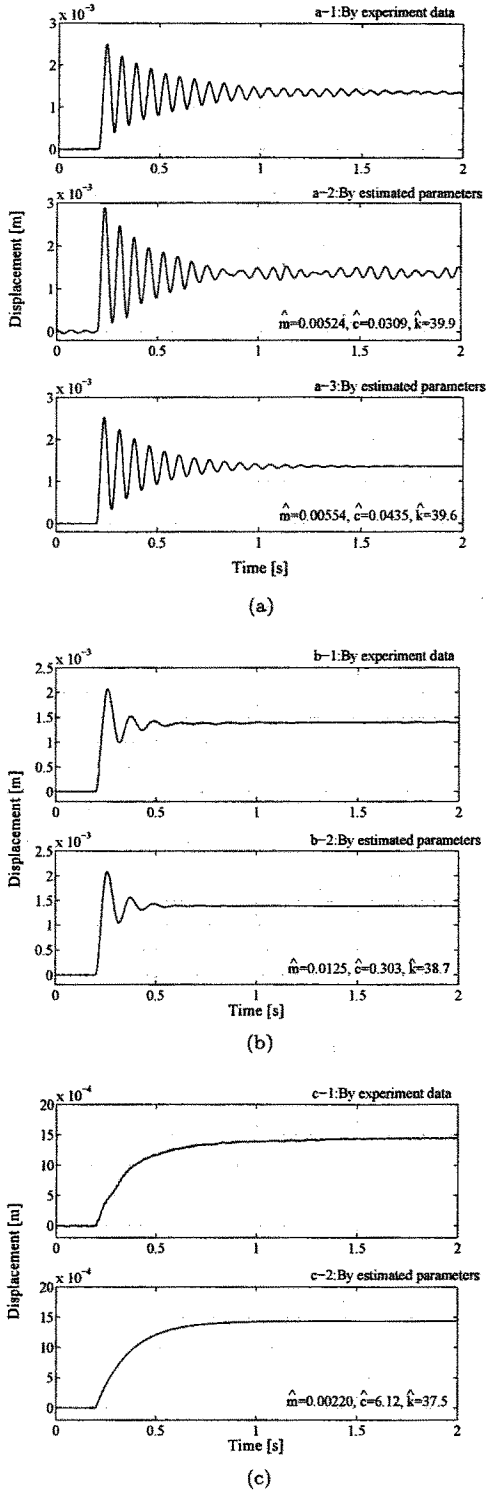

Fig. 7: Impedance estimation

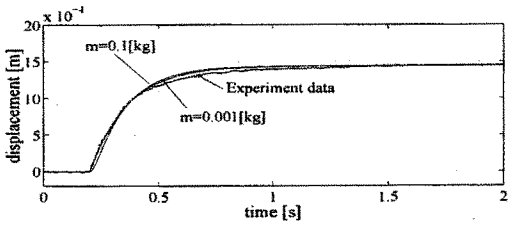

Fig. 8: Simulation

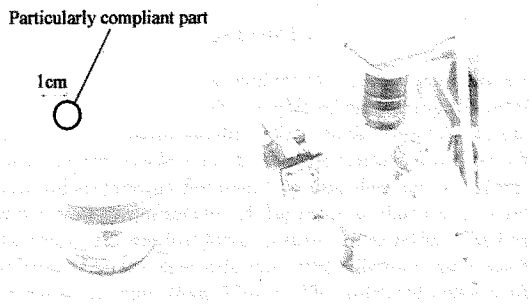

Fig. 9: Experimental setup for measuring the vibration characteristic of balloon

6 Concluding Remarks

This paper newly proposed a non-contact impedance estimation by utilizing air pressure, toward diagnosing an early stage of stomach cancer. We design and develop the prototype model for examining whether the system can successfully estimate the impedance parameter or not. The main results obtained through the work are summarized as follows: (1) The sensing system is mainly composed of a hose, an air compressor, and a solenoid valve with extremely high response. We can insert the hose into the hole equipped with an endoscope, which allows us to obtain the impedance sensing system with just a bit improvement. (2) Impedance measurement can be achieved within reasonable accuracy by utilizing the ideal step response of force and the output of distance sensor. (3) Experimental data show that stiffness can be nicely estimated for all responses, while mass is not especially under a strong damping.

Finally, we would like to express our sincere thanks for Mr. K. Kato and Mr. K. Tokuda for their strong supports in experiments and discussions.

References

[1] D.S. Kwon, K.Y. Woo, and H.S. Cho: Haptic control of the master hand controller for a microsurgical telerobot system, *In Proc. of the IEEE Int. Conf. on Robotics and Automation*, pp1722-1727, 1999

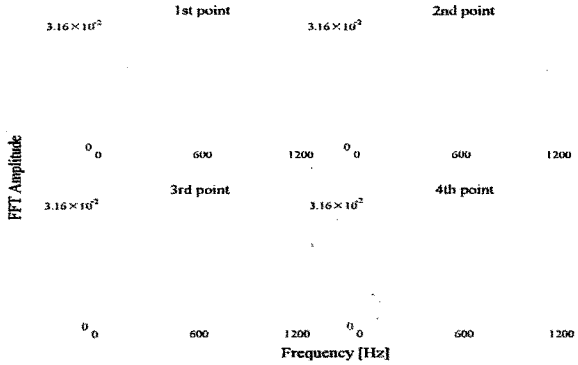

Fig. 10: FFT analysis

[2] A. Faraz and S. Payandeh: On inverse kinematics and trajectory planning for tele-laparoscopic manipulation, *In Proc. of the IEEE Int. Conf. on Robotics and Automation*, pp1734-1739, 1999

[3] M. Hayashibe and Y. Nakamura: Laser-poointing endoscope system for intra-operative 3D geometric registration, *In Proc. of the IEEE Int. Conf. on Robotics and Automation*, pp1543-1548, 2001

[4] H. Kang and J.T. Wen: Endobot - A robotic assistant in minimally invasive surgeries, *In Proc. of the IEEE Int. Conf. on Robotics and Automation*, pp2031-2037, 2001

[5] M. Ghodoussi, S.E. Butner, and Y. Wang: Robotic surgery - The transatlantic case, *In Proc. of the IEEE Int. Conf. on Robotics and Automation*, pp1882-1888, 2002

[6] F. Lai and R. Howe: Evaluting control modes for constrained robotic surgery, *In Proc. of the IEEE Int. Conf. on Robotics and Automation*, pp603-609, 2000

[7] R.A. Beasley and R.D. Howe: Tactile tracking of arteries in robotic surgery, *In Proc. of the IEEE Int. Conf. on Robotics and Automation*, pp3801-3806, 2002

[8] K. Ikuta, M. Takeuchi, and T. Namiki: Virtual endoscope system with force sensation, *In Proc. of the IEEE Int. Conf. on Robotics and Automation*, pp1715-1721, 1999

[9] N. Hogan: The mechanics of multi-joint posture and movement control, *Biol. Cybern.*, vol.53, pp1-17, 1985

[10] T. Tsuji, P.G. Morasso, K. Goto, and K. Ito: Human hand impedance characteristics during maintained posture, *Biol. Cybern.*, vol.72, pp475-485, 1995

[11] H. Shinoda and H. Yamasaki: Noncontact sensing of surface hardness, *J. of SICE*, vol.27, no.7, pp749-754, 1991

[12] H. Shinoda and H. Yamasaki: Noncontact sensing of surface hardness using pulsating air jet, *J. of SICE*, vol.28, no.10, pp1152-1159, 1992

[13] H. Schlighting: Boundary Layar Theory, *McGRAW-HILL BOOK COMPANY*, pp171-174, 1968

[14] S. Terasaki, N. Wada, N. Sakurai, N. Muramatsu, R. Yamamoto, and D.J. Nevins: Nondestructive mesurement of kiwifruit ripeness using a laser doppler vibrometer, *Transactions of the ASAE*, vol.44, no.1, pp81-87, 2001